CALIBRATION OF PARAMETERS FOR DISCRETE ELEMENT FRACTURED MODEL OF RICE STRAW AT THE APPROPRIATE HARVEST TIME
/
适收期水稻秸秆离散元可断裂模型参数标定

Jiang WANG
College of Automotive Engineering, Zibo Polytechnic University, Zibo/China;
Tel: 18801239355; E-mail: 12656@zbpu.edu.cn

DOI: https://doi.org/10.35633/inmateh-78-38

Keywords: *Rice straw; DEM calibration; Fracturable model; Optimal harvest period*

ABSTRACT

To address the lack of accurate and reliable straw models for simulating rice straw cutting, this study uses rice straw as the research object and constructs a discrete element model of straw using EDEM software to calibrate and optimize the bonding parameters. First, the physical parameters of rice straw were measured. For the bonding model parameters, a preliminary experiment was conducted to determine the range of bonding parameters, and the significance of each bonding parameter was analyzed using Plackett-Burman experiments to identify parameters with a significant impact on straw shear force. Then, a steepest climb test was conducted to determine the optimal combination of bonding parameters. Finally, a Box-Behnken simulation experiment was performed on the optimization interval, and a regression equation was established and solved to obtain the optimal parameter combination. The results show that the normal bonding stiffness, tangential bonding stiffness, and bonding radius have a significant impact on the straw shearing model. The optimal combination is 3.092×10¹⁰ Pa, 4.452×10¹⁰ Pa, and 0.496 mm. The established rice straw model is reliable and stable through multiple simulation experiments. This study provides an accurate and efficient method for optimizing the structure and motion parameters of rice straw crushing blades.

摘要

为解决水稻秸秆切断模拟过程缺乏准确可靠的秸秆模型，该研究以水稻秸秆为研究对象，利用 EDEM 软件构建秸秆离散元模型，对粘结参数进行标定与优化。首先对水稻秸秆物理参数进行了测定；针对粘结模型参数，先通过预试验确定模型粘结参数范围，并采用 Plackett-Burman 试验对各项粘结参数显著性进行分析，筛选出对秸秆剪切力影响大的参数，然后进行最陡爬坡试验，确定粘结参数最优组合所在区域范围，最后对优化区间进行 Box-Behnken 仿真试验，建立回归方程，求解获得最优参数组合。结果表明：法向粘结刚度、切向粘结刚度、粘结半径对秸秆剪切模型影响显著，最优组合为 3.092×10¹⁰Pa、4.452×10¹⁰Pa 和 0.496mm，并通过多次仿真试验验证建立的水稻秸秆模型可靠稳定，该研究可为优化水稻秸秆粉碎刀具结构和运动参数提供了准确高效方法。

INTRODUCTION

Returning rice straw to the field often requires cutting the straw to facilitate its spreading and decomposition. However, due to the large volume and toughness of the straw, incomplete pulverization can still occur. During the cutting process, the straw comes into contact with the pulverizing blades, leading to a complex interaction that directly impacts the machine's performance. Therefore, it is essential to study the characteristics of rice straw at the appropriate harvest time and its interaction with the pulverizing blades. This research is crucial for the design and optimization of key components used in returning straw to the field.

In recent years, an increasing number of domestic and international researchers have applied the Discrete Element Method (DEM) in agricultural engineering, establishing various flexible straw models and providing effective approaches for the development and optimization of related operating components. Lenaerts and Leblicq et al. constructed a segmented flexible straw model using DEM to simulate the straw–grain separation process in a harvester *(Bart et al., 2014; Leblicq et al., 2016)*. In this model, soft spheres are connected to form the flexible straw structure, and flexibility is achieved through springs $k_n$and dampers C_n connecting the spheres. *Wang Qirui et al* established a dynamic model considering the vibration response characteristics of flexible crop stalks to explore the separation mechanism of straw and analyze the process of grain separation (*Wang et al., 2020; Mao et al., 2020*). They also conducted a vibration response simulation. The straw model connects the particles through virtual bonds.

Liu Fanyi et al., (*2018*), established a wheat flexible straw model with a high degree of simulation. The model uses an empty cylinder as a template and is filled with multiple spheres. They studied and simulated the motion characteristics of the straw model in a horizontal airflow field. All the above studies have established flexible straw models, but they have not considered the fracture and breakage damage of straw. In order to more accurately and reliably simulate the root breakage process of corn stubble during deep loosening. *Liu,* (*2018*), established a fracturable root system model and conducted a straw shear calibration test. However, the root system model morphology is still quite different from the actual one and can only reflect a simple fracture morphology. *Liu et al.,* (*2020*), established a discrete element model of double-layer bonding, bimodal distribution of corn straw, and calibrated the mechanical parameters of the inner and outer layers of corn straw. However, corn straw and rice straw differ significantly, making it impossible to apply this model directly. In existing studies, the straw model and model parameters cannot meet the requirements of this study to reflect the stress fracture and breaking process of rice straw.

This paper focuses on rice straw harvested at the optimal time and examines its mechanical properties. The research utilizes the Hertz-Mindlin bonding model in EDEM to simulate the bonding of the straw. The ultimate shear force of the rice straw is used as the response variable for parameter calibration, and the reliability of the model is verified through simulation experiments. By establishing a reliable and accurate model of fractured rice straw, this study provides an effective approach for optimizing the structure and motion parameters of rice straw crushing tools.

MATERIAL AND METHODS

Determination of physical parameters of straw

The physical properties of straw primarily consist of external geometric dimensions, density, coefficient of restitution, and friction coefficient. The straw samples used in this study were sourced from the Longjing 31 rice variety, which is widely cultivated in Heilongjiang Province. Samples were collected from designated fields.

Geometric parameters

The geometric dimensions of rice straw primarily include length, outer diameter, and wall thickness. Although the diameter of the straw gradually decreases from the root to the panicle, the straw will break and become crushed when it is passed through the roller, resulting in a shorter straw length. The variation in diameter along the length is negligible, allowing the diameter to be treated as constant. For this study, one hundred straws collected from the roller at the time of rice harvest were randomly selected for measurement. Their geometric dimensions were assessed using vernier calipers.

Table 1 presents the measurement and analysis results of the geometric dimensions of straw. The data indicate that the coefficients of variation for both the outer diameter and wall thickness of rice straw are below 15%. This suggests that the variability in these two dimensions is low, making the average values suitable as representative measures. In contrast, the coefficient of variation for the measured length of the straw exceeds 15%, indicating a high degree of variability in size. Consequently, for subsequent simulations and analyses involving straw, it is advisable to select values within an appropriate range based on the specific conditions being simulated.

Table 1

Results of measurement and analysis of straw geometric dimensions

Size items	Maximum value / mm	Minimum value / mm	Average value / mm	Coefficient of variation / %
Length	550.26	98.31	364.19	26.38
Outer diameter	5.08	2.85	3.98	7.46
Wall thickness	0.49	0.38	0.45	6.24

Straw Density

The density of agricultural materials is commonly measured using liquid immersion and gas displacement methods (*Wang, 2021*). Due to its low density, straw's volume can be significantly influenced by the medium used during measurement (*Liu, 2018*). As a result, straw density is often expressed as mass per unit length. Since individual straw pieces have very small masses, measuring the mass of a single straw can lead to significant errors. To address this issue, five straw samples were randomly selected. The mass of each sample and the total length of the straw were measured to calculate the mass per unit length.

Table 2 presents the measurement results for the mass per unit length of straw. The average mass per unit length across the five samples was 2.14 × 10^{-3} g/mm. The coefficient of variation for the data was 3.15%, which is less than 15%. This indicates that the dispersion among the data is minimal, allowing the average value to effectively represent the mass per unit length of straw.

Table 2

Straw unit length mass measurement results

Items	1	2	3	4	5	Mean	Coefficient of variation / %
Mass per unit length / (×10^{-3} g/mm)	2.16	2.07	2.23	2.21	2.04	2.14	3.51

Straw Friction Parameters

The straw friction coefficient consists of both the static friction coefficient and the dynamic friction coefficient. During the straw feeding and crushing process in a straw feeding and crushing device, there is substantial relative motion occurring both among the straws themselves and between the straws and the working components of the device. Additionally, in discrete element modeling of straw, the interactions between particles are often characterized by friction. Therefore, accurately determining the friction coefficient is essential for subsequent analyses and for creating a reliable straw model.

The straw friction coefficient was measured using an MXD-01 friction coefficient measuring instrument, as illustrated in Figure 1. Figure 2 presents the test results for measuring the straw-steel plate friction coefficient. The straw sample was cut to a suitable length and evenly adhered to the lower surface of the test slider. Meanwhile, the upper surface of the lower steel plate (65Mn) was kept clean. Following the test, the instrument automatically displayed the static friction coefficient, which was recorded. To determine the straw-steel plate dynamic friction coefficient, the straw was evenly distributed over the upper surface of the lower steel plate. In contrast, the lower surface of the test slider remained untreated. After the test, the dynamic friction coefficient was displayed by the instrument and recorded. For measuring the straw-straw static friction coefficient, the straw was adhered to both the lower surface of the test slider and the upper surface of the lower steel plate. When evaluating the straw-straw dynamic friction coefficient, the straw was attached to the lower surface of the test slider. In contrast, additional straw was spread over the upper surface of the lower steel plate. All other procedures remained consistent with the previous tests. Each set of tests was conducted five times, and the relevant data are presented in Table 3. The data indicate that the coefficients of variation for all measurements are less than 15%, allowing the average values to be used to represent the test results.

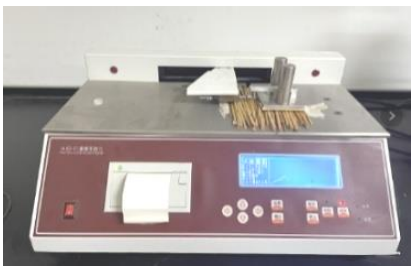

Fig. 1 - MXD-01 Friction Coefficient Measuring Instrument

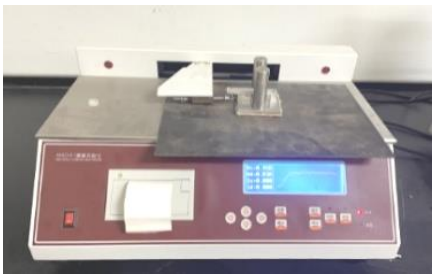

Fig. 2 - Test results

Table 3

Test results of straw friction coefficients

Items	Maximum value	Minimum value	Average value	Coefficient of variation / %
Static friction coefficient between straw and steel plate	0.79	0.63	0.71	7.76
Dynamic friction coefficient between straw and steel plate	0.27	0.12	0.18	13.44
Static friction coefficient between straw particles	0.55	0.38	0.49	13.05
Dynamic friction coefficient between straw particles	0.14	0.04	0.08	11.95

Collision Rejuvenation Coefficient

The collision rejuvenation coefficient measures the ability of straw to return to its original shape after a collision. A higher coefficient signifies a greater capacity for the straw to regain its form. During the processes of crushing and spreading straw, many collisions and compressions take place both between the straws and between the straws and the working components. Establishing the appropriate collision rejuvenation coefficient is essential for accurately calculating the forces in subsequent simulations.

The collision rejuvenation coefficient is defined as the ratio of the normal velocity of the object after the collision to its normal velocity before the collision (*Lu et al., 2016; Huang et al., 2014; Liu et al., 2025*). The calculation formula is as follows:

$$e = \frac{v_{h_1}}{v_{H_1}} = \frac{\sqrt{2gh_1}}{\sqrt{2gH_1}} = \sqrt{\frac{h_1}{H_1}} \quad (1)$$

In the formula, v_{h1} and v_{H1} are the velocities of the two objects after the collision, m/s; h_1 and H_1 are the bounce height and release height, m.

According to formula (1), the coefficient of restitution of straw in this paper is calculated by the ratio of bounce height to release height. However, the straw length is relatively large. If the release height of the straw is large, it will be greatly affected by air resistance, but if it is too small, the rebound effect will not be obvious. In order to ensure the accuracy of the measurement, the release height of straw is determined to be 350 mm according to relevant literature (*Wang., 2021*). The straw coefficient of restitution test platform shown in Figures 3 and 4 is established to determine the straw coefficient of restitution. When determining the straw-straw coefficient of restitution, multiple straws are glued to the surface of the cardboard. The surface should be flat to serve as the straw rebound surface. After setting it up, the straw is dropped freely from the preset height, and a high-speed camera records the descent process. When determining the coefficient of restitution of the straw-steel plate, the rebound surface of the straw was replaced with a steel plate, and other treatments were the same as those in the above determination. To avoid randomness, each group of experiments was repeated 10 times. Finally, the rebound height h1 of the straw in each experiment was determined by taking pictures.

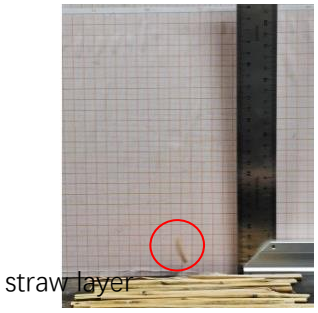

Fig. 3 - Determination of straw-straw coefficient of restitution

Fig. 4 - Determination of the coefficient of restitution between straw and steel plate.

Table 4 presents the results of the measurement of the straw coefficient of restitutions. The coefficients of variation for both measurements are below 15%, which indicates that the results from multiple tests are relatively consistent. Therefore, the average value can be considered the final measurement result. The measured coefficient of restitution for straw-straw collisions is 0.30, while the coefficient of restitution for straw-steel plate collisions is 0.33.

Table 4

Results of straw coefficient of restitution measurements

Items	Maximum value	Minimum value	Average value	Coefficient of variation/%
Straw-to-straw coefficient of restitution	0.38	0.26	0.30	10.55
Straw-to-steel plate coefficient of restitution	0.39	0.28	0.33	9.43

Model Construction

Based on the geometric parameters of rice straw, the outer diameter of the straw model is 3.98 mm, and the average wall thickness is 0.45 mm. Real rice straw has relatively thin walls; if particles reflecting the actual wall thickness were used in the model, they would be very small and densely distributed, resulting in excessive computational demands. Therefore, in the simulation model, the wall thickness of the straw was appropriately increased while maintaining the outer diameter at 3.98 mm. Consequently, the inner diameter was set to 1.98mm.

The modeling process is outlined as follows. First, a three-dimensional model of rice straw was created using SolidWorks 2018 and saved as an STL file. The length of the straw model was set to 80 mm. Next, the 3D straw model was imported into EDEM 2018 and defined as a virtual model. Particles were then generated based on the imported model, which served as the particle factory. To accurately represent the straw structure and simulate its mechanical behavior, the radius of the filling particles was set to 0.35 mm. To facilitate stable bond generation during the simulation, the contact radius was adjusted to 120% of the particle radius, resulting in a value of 0.42 mm. The particle generation mode used in this process was static generation. The final configuration of the straw model and its particle filling is illustrated in Fig. 5.

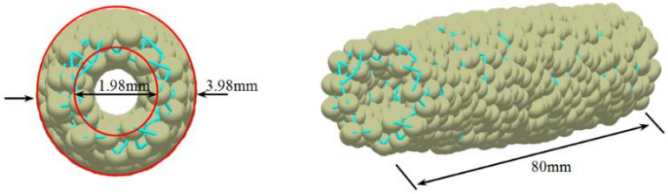

Fig. 5 - Straw model and particle filling configuration

Density Calibration

In the discrete element method (DEM) modeling process for straw, individual particles must be bonded together to represent the straw structure. Because the modeling configuration differs from that of real straw, the straw density must be recalibrated. The particle density was adjusted during parameter setting until it matched the measured mass per unit length of straw, *m_d*, satisfying Eq. (2).

$$m_d = \frac{m_r}{l_r} \quad (2)$$

where m_r is the mass of the straw model (g); l_r is the length of the straw model (mm).

In the previous section, the measured mass per unit length of straw, m_d, was 2.14 × 10^{-3} g/mm. The straw length l_r in the simulation model was 80 mm, yielding a simulated straw mass m_r of 0.17 g. After conversion, the calibrated particle density of the straw model was determined to be 227 kg/m³.

Bonding Parameter Calibration

A universal testing machine was used to evaluate the cutting behavior of straw. After multiple tests, the maximum shear force of the straw was determined to be 35.68 N (with the shear speed set to 240 mm/min). The experimental equipment and the cutting results are shown in Fig. 6. In the EDEM software, the established flexible and breakable straw model was used to simulate the actual cutting process. The two ends of the straw model were fixed to ensure zero displacement at both ends, and the simulated cutting speed was kept consistent with the experimental value of 240 mm/min. A straw shear simulation model corresponding to the actual shear test was established, as shown in Fig. 7.

Fig. 6 - Actual straw shear test

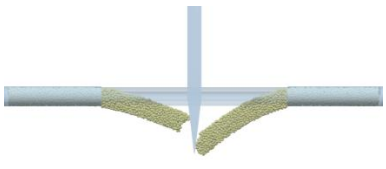

Fig. 7 - Straw shearing simulation model

The basic parameters of model particles within the Hertz-Mindlin with bonding contact model are classified into three categories: intrinsic parameters, contact parameters, and bonding parameters. Through reference studies and extensive simulations involving shearing adjustments (*Jia et al., 2021; Li., 2011; Ding et al., 2017; Hou et al., 2022; Liao et al., 2020; Mi et al., 2025*), the essential parameters for the straw model particles were identified, as detailed in Table 5.

Table 5

Basic parameters of straw model pellets

items	Simulation Parameters	Parameter Values
Self-parameters	Steel density/(kg·m^{-3})	7800
	Straw density/(kg·m^{-3})	7.9
	Steel Poisson's ratio	0.3
	Straw Poisson's ratio	0.4
	Steel shear modulus/MPa	7.9×104
	Straw shear modulus/MPa	1
Contact parameters	Straw-steel coefficient of restitution	0.33
	Straw-steel static friction coefficient	0.71
	Straw-steel kinetic friction coefficient	0.18
	Straw-straw complex coefficient	0.30
	Straw-straw static friction coefficient	0.49
	Straw-straw kinetic friction coefficient	0.08
Bonding parameters	Normal bond stiffness (N·m^{-3})	1×10^{10}~9×10^{10}
	Tangential bond stiffness (N·m^{-3})	1×10^{10}~1×10^{10}
	Normal critical stress/Pa	1.5×10^{11}~1.5×10^{13}
	Tangential critical stress/Pa	1×10^{11}~1×10^{13}
	Bond radius/mm	0.35-0.70

Straw shear simulation requires determining five basic bonding parameters; however, not every parameter significantly affects the shear resistance of straw. To enhance the efficiency of subsequent optimization experiments, Plackett-Burman tests are necessary for these five parameters.

The list of test parameters was developed using Design-Expert 13.0, as presented in Table 6. Each parameter group was assigned two levels, coded as 1 and -1, respectively. A total of twelve simulation experiments were conducted with varying parameter levels to meet the specified requirements.

Table 6

List of Plackett-Burman simulation test parameters

Parameters	Parameter Encoding	Parameter Level	
		Low Level (-1)	High Level (1)
Normal bond stiffness / (N·m^{-3})	X1	1×10^{10}	9×10^{10}
Tangential bond stiffness / (N·m^{-3})	X2	1×10^{10}	9×10^{10}
Normal critical stress / Pa	X3	1.5×10^{11}	1.5×10^{13}
Tangential critical stress / Pa	X4	1×10^{11}	1×10^{13}
Bond radius / mm	X5	0.35	0.70

RESULTS

Results of Plackett-Burman test

The design and results of the Plackett-Burman test are shown in the table 7.

Table 7

Results of Plackett-Burman simulation experiments

Test number	X1	X2	X3	X4	X5	Ultimate shear force (F_m) / N
1	1	1	-1	1	1	72.60
2	-1	1	1	-1	1	27.20
3	1	-1	1	1	-1	5.89
4	-1	1	-1	1	1	16.07
5	-1	-1	1	-1	1	16.93
6	-1	-1	-1	1	-1	5.77
7	1	-1	-1	-1	1	40.07
8	1	1	-1	-1	-1	21.30

Test number	X1	X2	X3	X4	X5	Ultimate shear force (F_m) / N
9	1	1	1	-1	-1	36.64
10	-1	1	1	1	-1	9.31
11	1	-1	1	1	1	37.9
12	-1	-1	-1	-1	-1	4.73

An analysis of variance was conducted on the simulation results using Design-Expert 13 software, with the significance of each parameter presented in Table 8. The findings indicate that the order of influence of the five bonding parameters on the maximum shear force of straw is as follows: X1 > X5 > X2 > X3 > X4. To streamline the subsequent experiments without compromising simulation accuracy, only the top three factors affecting the maximum shear force were selected for further analysis. These factors are the normal bonding stiffness (X1), tangential bonding stiffness (X2), and bonding radius (X5).

Table 8

Significance Analysis of Plackett-Burman Simulation Experiments

Source	Effect	Standard Error	Sum of Squares	F	P	Significance Ranking
Model		0.289	3341.17	3.98	0.0612	
X1	22.398	0.289	1505.06	8.97	0.0241*	1
X2	11.971	0.289	429.96	2.56	0.1605	3
X3	-4.445	0.289	59.27	0.35	0.5739	4
X4	0.1116	0.289	0.037	0.0002	0.9886	5
X5	21.188	0.289	1346.84	8.03	0.0298*	2

* indicates a significant effect at the 0.05 level.

Results of the Steepest Ascent Test

To further narrow the range of each simulation parameter and quickly identify the optimal values, a steepest ascent test was conducted on the factors determined by the Plackett–Burman test. The experimental design and simulation results of the steepest ascent test are presented in Table 9. For serial numbers 2 and 3 in the steepest ascent test, the corresponding parameter ranges were as follows: the normal bond stiffness ranged from 3×10^{10} to 5×10^{10} Pa, the tangential bond stiffness ranged from 3×10^{10} to 5×10^{10} Pa, and the bond radius ranged from 0.45 to 0.55 mm.

Table 9

Factor levels and simulation results for the steepest climb test

Number	Normal Bond Stiffness (X1) / Pa	Tangential Bond Stiffness (X2) / Pa	Bond Radius (X5) / mm	Ultimate Shear Force / N
1	1×1010	1×10^{10}	0.35	3.54
2	3×1010	3×10^{10}	0.45	10.79
3	5×1010	5×10^{10}	0.55	47.90
4	7×1010	7×10^{10}	0.65	56.60
5	9×1010	9×10^{10}	0.70	102.11

Results of the Box-Behnken Simulation

After determining the appropriate range for each parameter through the steepest ascent test, the next step was to identify the optimal parameter combination to achieve a flexible straw model consistent with the actual shearing behavior. Therefore, a Box–Behnken experimental design was conducted. The factor level settings of the experiment are presented in Table 10, while the results of the Box–Behnken experimental design are shown in Table 11.

Table 10

Box-Behnken Test Levels

factor	level		
	low (-1)	medium (0)	high (1)
Normal bond stiffness / Pa	3×10^{10}	4×10^{10}	5×10^{10}
Tangential bond stiffness / Pa	3×10^{10}	4×10^{10}	5×10^{10}
Bond radius / mm	0.45	0.50	0.55

Table 11

Box-Behnken Experimental Design and Results

Number	Normal bond stiffness (X1) / Pa	Tangential bond stiffness (X2) / Pa	Bond radius (X5) / mm	F_m / N
1	-1	-1	0	11.96
2	1	-1	0	25.27
3	-1	1	0	29.31
4	1	1	0	17.17
5	-1	0	-1	24.83
6	1	0	-1	27.45
7	-1	0	1	20.94
8	1	0	1	22.95
9	0	-1	-1	34.22
10	0	1	-1	38.57
11	0	-1	1	34.24
12	0	1	1	33.61
13	0	0	0	52.27
14	0	0	0	52.61
15	0	0	0	52.98

The results of the Box-Behnken test were analyzed using a quadratic polynomial regression to derive the equation relating the simulated ultimate shear force (Fm) of flexible, breakable rice straw to the experimental parameters.

$$F_m = 52.62 + 0.73X_1 + 1.62X_2 - 1.67X_5 - 6.36X_1X_2 - 0.15X_1X_5 - 1.25X_2X_5 - 2.41X_1^2 - 10.29X_2^2 - 7.17X_5^2 \quad (3)$$

ANOVA (Analysis of Variance) was conducted on the model, and the results are detailed in Table 12. The table indicates that the quadratic terms for normal bond stiffness, tangential bond stiffness, and bond radius have highly significant effects on the simulated experimental response values. Additionally, tangential bond stiffness and bond radius significantly influence the response values, while the other terms do not show a significant impact. The ANOVA results reveal a P-value of less than 0.0001 for the model, signifying a highly significant relationship between the model and each variable. In contrast, the lack-of-fit term has a P-value of 0.0531, which is greater than 0.05, suggesting that the model is not influenced by other factors and there are no lack-of-fit concerns. Moreover, the coefficient of determination (R^2) and the adjusted coefficient of determination (R^2a) for the regression model are 0.9969 and 0.9913, respectively. Both values are close to 1, indicating a strong fit between the model and the actual measured values, reflecting high reliability of the model.

Table 12

Analysis of Variance of Experimental Regression Model

Sources of variance	Sum of squares	Degrees of freedom	*F*	*P*
Model	2274.67	9	179.02	<0.0001*
X1	4.20	1	2.98	0.1450
X2	21.03	1	14.89	0.0119*
X5	22.21	1	15.73	0.0107*
X1 X2	161.93	1	114.69	0.0001*
X1 X5	0.0930	1	0.0659	0.8076
X2 X5	6.20	1	4.39	0.0903
X12	1691.72	1	1198.26	<0.0001*
X22	390.77	1	276.78	<0.0001*
X52	189.95	1	134.54	<0.0001*
Residual	7.06	5		
Misfit Term	6.81	3	17.99	0.0531
Pure Error	0.2522	2		
Sum	2281.73	14		

* indicates a significant effect at the 0.05 level.

Using the measured ultimate shear force of rice straw (35.68 N) as the target value, the optimization module of Design-Expert 13 software was used to solve the quadratic regression model. The optimal values for the normal bond stiffness, tangential bond stiffness, and bond radius were determined to be 3.092 × 10^{10} Pa, 4.452 × 10^{10} Pa, and 0.496 mm, respectively. The remaining bond parameters were kept consistent with those established in the steepest ascent test.

Simulation Verification

To confirm the accuracy of the optimized bonding parameters, simulation verification experiments were conducted using the specified parameter combinations. To minimize experimental variability, each experiment was repeated three times, resulting in simulated ultimate shear forces of 35.01 N, 36.07 N, and 36.21 N, respectively. The errors compared to the actual measured results were 1.88%, 1.09%, and 1.49%. Overall, the experimental results closely aligned with the physically measured values. As depicted in Figure 10, although there are some differences between the simulated and measured curves, the overall trends are consistent, further validating the model's reliability and accuracy.

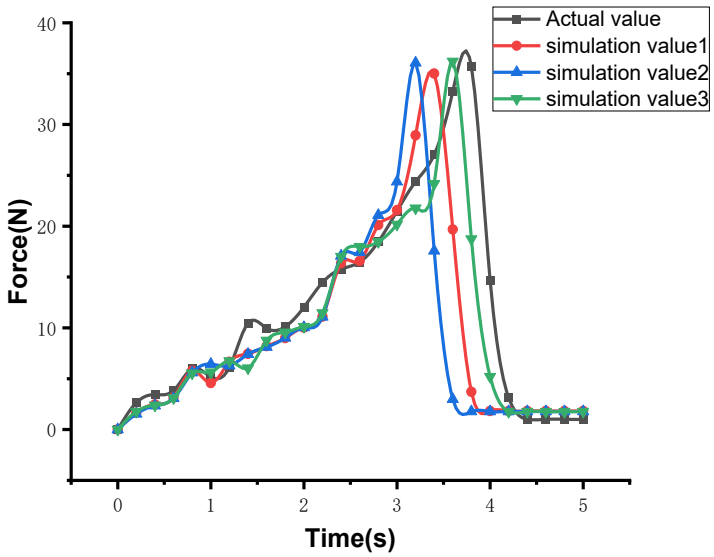

Fig. 8 - Comparison of time-load curves between simulated mechanical experiments and actual tests

CONCLUSIONS

This paper investigated the physical properties of rice straw from Northeast China and developed a flexible, fracturable straw model using EDEM. The following conclusions were drawn:

1. Measurements of the straw's geometric dimensions after threshing indicated that the average length, outer diameter, and wall thickness were 364.19 mm, 3.98 mm, and 0.45 mm, respectively. The average mass per unit length of the straw was found to be 2.14 × 10^{-3} g/mm. Additionally, the average coefficients of restitution for straw-straw and straw-steel plate collisions were 0.30 and 0.33, respectively. The average static and dynamic friction coefficients for the straw against the steel plate were 0.71 and 0.38, while the straw-straw coefficients were 0.49 and 0.28, respectively. The maximum average shear force of the straw was measured at 35.68 N.

2. The Plackett-Burman test was utilized to identify the bonding parameters that significantly influence the ultimate shear force of the straw: normal bonding stiffness, tangential bonding stiffness, and bonding radius. Subsequently, the steepest ascent method was employed to further refine the range of these three bonding parameters. Finally, the Box-Behnken test was conducted to determine the optimal combination of bonding parameters when the ultimate shear force is 35.68 N. The optimal values for normal bonding stiffness, tangential bonding stiffness, and bonding radius were found to be 3.092×10^{10} Pa, 4.452×10^{10} Pa, and 0.496 mm, respectively.

3. Simulation experiments showed that, under optimized parameter combinations, the errors between the ultimate shear force of straw and the actual measured results were 1.88%, 1.09%, and 1.49%, respectively, verifying the accuracy of the model.

REFERENCES

[1] Bart L., Thomas A., Engelbert T., Ketelaere D., Herman R., Josse B.D., Wouter S. (2014). Simulation of grain–straw separation by Discrete Element Modeling with bendable straw particles. *Computers and Electronics in Agriculture*, 101(C), pp.24-33, DOI: http://dx.doi.org/10.1016/j.compag.2013.12.002.

[2] Ding Q.S., Ren J., Adam B.E., Zhao J.K., Ge S.Y., Li Y. (2017). DEM Analysis of Subsoiling Process in Wet Clayey Paddy Soil (湿粘水稻土深松过程离散元分析). *Transactions of the Chinese Society of Agricultural Machinery*, 48(3), pp. 38-48, DOI: 10.6041/j.issn.1000-1298.2017.03.005.

[3] Huang X.M., Zha X.T., Pan H.B., Zong W,Y.,Chen H. (2014). Measurement and analysis of rapeseeds' restitution coefficient in point-to-plate collision model (油菜籽粒点面接触碰撞中恢复系数的测定及分析). *Transactions of the Chinese Society of Agricultural Engineering*, 30(24), pp.22-29, DOI:10.3969/j.issn.1002-6819.2014.24.003.

[4] Hou J., Xie F.P., Wang X.S., Liu D.W., Chen Z.G. (2022). Measurement of contact physical parameters of flexible rice straw and discrete element simulation calibration (水稻茎秆接触物理参数测定与离散元仿真标定). *Acta Agriculturae Universitatis Jiangxiensis*, 44(3), pp. 747-758, DOI: 10.13836/j.jjau.2022074.

[5] Jia H.L., Deng J., Deng Y.L., Chen T.Y., Wang G., Sun Z.J., Guo H. (2021) Contact parameter analysis and calibration in discrete element simulation of rice straw. *International journal of agricultural and biological engineering*, 14(03), pp. 72-81, 10.25165/IJABE.V14I4.6435.

[6] Leblicq T., Smeets B., Ramon H., Saeys W. (2016). A discrete element approach for modelling the compression of crop stems. *Computers and Electronics in Agriculture*, 123(C), pp.80-88, DOI: http://dx.doi.org/10.1016/j.compag.2016.02.018.

[7] Li H.C. (2011). *Theoretical and Experimental Research on Wind Sieve Cleaning Device* (风筛式清选装置理论及试验研究), PhD dissertation, Jiangsu University.

[8] Liao Y.C., Liao Q.X., Zhou Y., Wang Z.T., Jiang Y.J., Liang F. (2020). Parameters Calibration of Discrete Element Model of Fodder Rape Crop HarVest in Bolting Stage (饲料油菜薹期收获茎秆破碎离散元仿真参数标定). *Transactions of the Chinese Society of Agricultural Machinery*, 51(6), pp. 73-82, DOI: 10.6041/j.issn.1000-1298.2020.06.008.

[9] Liu C.Y., Zhang F.W., Song X.F., Wang F., Zhang F.Y., Li X.Z., Cao X,Q. (2020). Study on mechanical properties for corn straw of double-layer bonding model based on discrete element method (基于离散元法玉米秸秆双层粘结模型力学特性研究). *Journal of Northeast Agricultural University*, 53(1), pp. 45-54, DOI: 10.19720/j.cnki.issn.1005-9369.2022.01.006.

[10] Liu F., Zhang J., Chen J. (2018). Modeling of flexible wheat straw by discrete element method and its parameters calibration. *International Journal of Agricultural and Biological Engineering*, 11(03), pp. 42-46, DOI:10.25165/j.ijabe.20181103.3381.

[11] Liu F.Y. (2018). *Study on Discrete Element Modeling of Wheat Grains and Short Straw in the Cleaning Device* (清选装置中小麦颗粒和短茎秆离散元建模研究), PhD dissertation, Northwest A&F University.

[12] Liu J.A. (2018). *Study on Parameter Optimization of Deep Subsoiler and Comprehensive Soil Loosening Effects Based on Discrete Element Method* (基于离散元方法的深松铲参数优化及松土综合效应研究), PhD dissertation, China Agricultural University.

[13] Liu X.Y., Wang C., Shao Y.C., Zhang W.J. (2025). Discrete Element Modeling and Parameter Calibration for Corydalis Tuber. *INMATEH-Agricultural Engineering*, 76(2), pp.26-37, DOI: https://doi.org/10.35633/inmateh-76-02.

[14] Lu Y.G., Wu N., Wang B., Yu Z.Y., Lin D.Z., Hu Z.C. (2016). Measurement and analysis of peanuts' restitution coefficient in point-to-plate collision mode (花生荚果碰撞模型中恢复系数的测定及分析). *Journal of China Agricultural University*, 21(8), pp. 111-118, DOI: 10.11841/j.issn.1007-4333.2016.08.15.

[15] Mao H., Wang Q., Li Q.L. (2020). A discrete element approach for modelling bendable crop stems. *Computers and Electronics in Agriculture*, 170(C), pp. 105229, DOI: https://doi.org/10.1016/j.compag.2020.105229.

[16] Mi J., Xie H., Niu P. (2025). Design And Optimisation of Rotary Tiller Blade for Orchards in Hilly Mountainous Areas Based on the Discrete Element Method. *INMATEH-Agricultural Engineering*, 76(2), pp.177-186, DOI: https://doi.org/10.35633/inmateh-76-16.

[17] Ren J.H., Wu T., Liu Q.T., Mo W.Y.J., Li K. (2022). Discrete element simulation modeling method and parameter calibration of sugarcane segment (蔗段离散元仿真建模方法与参数标定). *Journal of South China Agricultural University*, 43(3), pp. 124-132, DOI: http://dx.doi.org/10.7671/j.issn.1001-411X.202108015.

[18] Wang H.Y. (2021). *Research on the Stress Transmission Law of Alfalfa Straw Vibration Compression Based on Discrete Element Method* (基于离散元法的苜蓿秸秆振动压缩过程热及应力传递研究), Master Thesis, Inner Mongolia Agricultural University.

[19] Wang Q.R., Mao H.P., Li Q.L. (2020). Simulation of Vibration Response of Flexible Crop Stem Based on Discrete Element Method (基于离散元的柔性作物茎秆振动响应仿真). *Transactions of the Chinese Society of Agricultural Machinery*, 51(11), pp. 131-137, DOI: 10.6041/j.issn.1000-1298.2020.11.014.

[20] Wang Z.D. (2021). *Design and experiment of key components for corn threshing with longitudinal axial flow and variable diameter threshing rod* (玉米纵轴流纹杆式变径脱粒关键部件的设计与试验), PhD dissertation, China Agricultural University.

[21] Zhang W.F., Song X.F., Zhang X.K., Zhang F.Y., Wei W.C., Dai F. (2019). Simulation and experiment on mechanical characteristics of kneading and crushing process of corn straw (玉米秸秆揉丝破碎过程力学特性仿真与试验). *Transactions of the Chinese Society of Agricultural Engineering*, 35(9), pp. 58-65, DOI: 10.11975/j.issn.1002-6819.2019.09.007.